A Theoretical Study of the Heck Reaction: *N*-Heterocyclic Carbene versus Phosphine Ligands

Ming-Tsung Lee, Hon Man Lee, and Ching-Han Hu*

Department of Chemistry, National Changhua University of Education, Changhua 50058, Taiwan, Republic of China

Received July 18, 2006

The reaction mechanism of the Heck reaction has been studied using theoretical chemistry. Our main focus has been the comparison between phosphine ligands and *N*-heterocyclic carbenes (NHC) and between the normal C2-NHC versus the "abnormal" C5-NHC. Our overall free-energy landscape shows that oxidative addition involves a significant energy barrier, while the phosphine system is relatively favored. In the olefin insertion and β-hydride elimination steps, we considered both the neutral and ionic pathways. For the ionic pathway, the rate-determining step in addition to oxidative addition is olefin migration. For the neutral pathway, the second rate-determining step in addition to oxidative addition is also olefin insertion for NHC systems, while for the phosphine system the energy profile is much flatter. For the phosphine system, our result suggests that the neutral pathway is favored. Our study demonstrates that the catalytic capacity of Pd^0L_2 involving the "abnormal" C5-NHC ligand is comparable to the regular C2-NHC ligand. For the mechanisms examined in this study, there is no obvious advantage of using NHC ligands.

1. Introduction

The Heck reaction was reported in the late 1960s as a new method for C−C bond formation.[1] Since the first discovery of the Heck reaction, the development of its applications in various coupling reactions has attracted the attention of chemists and has been summarized in several reviews.[2−5] It is generally recognized that Pd^0 coordinated with weak donors such as tertiary phosphines is the catalytically active species.[3] A common approach is to begin with Pd^{II} salts such as $Pd^{II}(OAc)_2$, followed by in situ reduction. An alternative mechanism involving a Pd^{IV} species was proposed by Herrmann et al.[6] The proposal was spurred by the discovery of a Pd^{IV} complex,[7] and the mechanism has been investigated by Martin et al. using theoretical methods.[8] Herrmann et al. have demonstrated that palladacycles are well-defined, efficient catalysts or precursors for Heck coupling reactions.[9]

A simplified description of the Heck reaction is shown in Scheme 1, and the catalytic cycle is often referred to as the "classical" mechanism. The mechanism consists of four parts: oxidative addition, olefin insertion, β-hydride elimination, and base elimination. At the second step (olefin insertion), the reaction can occur via either neutral or cationic pathways (as shown in Scheme 1). In the neutral pathway, originally proposed by Heck,[10] a phosphine ligand is dissociated from the complex prior to olefin coordination, while in the cationic pathway, first proposed by Cabri et al.,[11] the bromide ion is dissociated. Monoligated Pd^0L has been proposed as the catalytic species that undergoes oxidative addition;[12] however this mechanism is not considered in this study.

Since the Arduengo et al.[13] isolation of stable *N*-heterocyclic carbenes (NHCs) in 1991, preparations of NHC have become accessible to chemists.[13,14] Owing to their extraordinary properties, NHC ligands have been found to be involved in a great variety of catalytic processes.[15−18] Studies toward the applications of NHC ligands in organometallic chemistry have intensified in the past few years. Recent progress in the preparations of NHC complexes has also accelerated the development and application of NHC-based catalysts in a variety of organic reactions.[17,19] In ruthenium-catalyzed olefin metathesis reactions, the replacement of one phosphine ligand in the conventional bis-phosphine ruthenium catalyst (known as the first-generation Grubbs catalyst) significantly increases the catalytic activity.[20,21] Moreover, the phosphine ligands have been, in part, replaced by NHCs due to their demonstrated excellence in homogeneous catalysis. Herrmann referred to the fast development of NHC

(1) Heck, R. F. *J. Am. Chem. Soc.* **1968**, *90*, 5518−5526.
(2) Cabri, W.; Candiani, I. *Acc. Chem. Res.* **1995**, *28*, 2−7.
(3) de Meijere, A.; Meyer, F. E. *Angew. Chem., Int. Ed.* **1994**, *33*, 2379−2411.
(4) Crisp, G. T. *Chem. Soc. Rev.* **1998**, *27*, 427−436.
(5) Dupont, J.; Pfeffer, M.; Spencer, J. *Eur. J. Inorg. Chem.* **2001**, 1917−1927.
(6) Böhm, V. P. W.; Herrmann, W. *A. Chem.−Eur. J.* **2001**, *7*, 4191−4197.
(7) Canty, A. J. *Acc. Chem. Res.* **1992**, *25*, 83−90.
(8) Sundermann, A.; Uzan, O.; Martin, J. M. L. *Chem.−Eur. J.* **2001**, *7*, 1703−1711.
(9) Herrmann, W. A.; Brossmer, C.; Reisinger, C.-P.; Riermeier, T. H.; Öfele, K.; Beller, M. *Chem.−Eur. J.* **1997**, *3*, 1357−1364.
(10) Heck, R. F. *Acc. Chem. Res.* **1979**, *12*, 146−151.
(11) Cabri, W.; Candiani, I.; Bedeschi, A. *J. Org. Chem.* **1993**, *58*, 7421−7426.
(12) Christmann, U.; Vilar, R. *Angew. Chem., Int. Ed.* **2005**, *44*, 366−374.
(13) Arduengo, A. J., III; Harlow, R. L.; Kline, M. *J. Am. Chem. Soc.* **1991**, *113*, 361−363.
(14) Regitz, M. *Angew. Chem., Int. Ed.* **1996**, *35*, 725−728.
(15) Herrmann, W. A.; Köcher, C. *Angew. Chem., Int. Ed.* **1997**, *36*, 2162−2187.
(16) Weskamp, T.; Böhm, V. P. W.; Herrmann, W. A. *J. Organomet. Chem.* **2000**, *600*, 12−22.
(17) Herrmann, W. A. *Angew. Chem., Int. Ed.* **2002**, *41*, 1290−1295.
(18) Trnka, T. M.; Grubbs, R. H. *Acc. Chem. Res.* **2001**, *34*, 18−29.
(19) Kremzow, D.; Seidel, G.; Lehmann, C. W.; Fürstner, A. *Chem.−Eur. J.* **2005**, *11*, 1833−1853.
(20) Sanford, M. S.; Love, J. A.; Grubbs, R. H. *J. Am. Chem. Soc.* **2001**, *123*, 6543−6554.
(21) Trnka, T. M.; Morgan, J. P.; Sanford, M. S.; Wilhelm, T. E.; Scholl, M.; Choi, T. L.; Ding, S.; Day, M. W.; Grubbs, R. H. *J. Am. Chem. Soc.* **2003**, *125*, 2546−2558.

10.1021/om060651p CCC: $37.00
Publication on Web 02/08/2007

Scheme 1

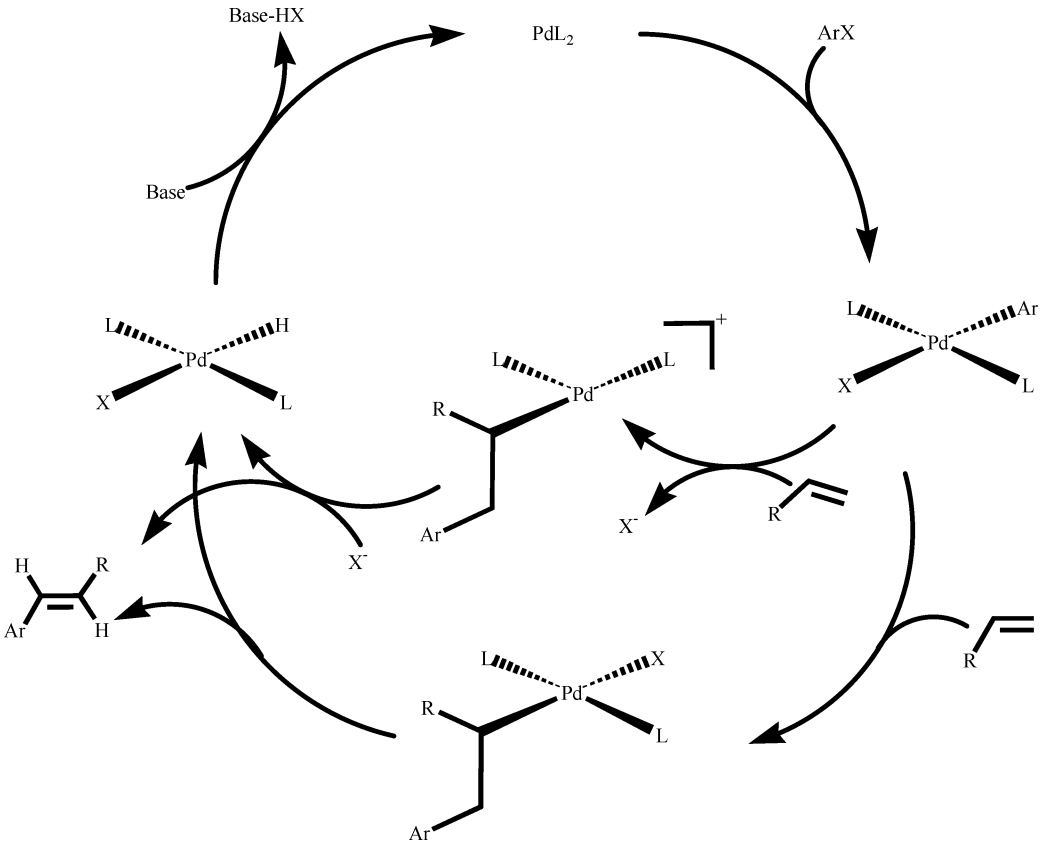

as "a revolutionary turning point in organometallic catalysis".[17] Recently, there have been several reports on the application of NHC ligands in the Heck reaction.[19,22−26]

The complex mechanism of the Heck reaction has posed a challenge to both experimental and computational chemists.[8,27−35] Most of the investigations have involved the Pd^0/Pd^{II} reactions rather than Pd^{II}/Pd^{IV} reactions. A series of mechanistic studies by Amatore et al. led to the conclusion that $L_2Pd^0X^-$, instead of Pd^0L_2, is the catalytic species.[32] In this mechanism, the product of oxidative addition is a five-coordinate complex, and in the final stage, the full catalytic cycle is completed by removing a proton (instead of HX) from the $L_2Pd^0X^-$ complex. Most of the theoretical studies mentioned above used model phosphine ligands, with the exception of the research of Albert et al., in which the authors studied the insertion and elimination steps of the reaction using model NHC compounds.[27] Interestingly the authors used a bidentate ligand, consisting of an NHC and a phosphine moiety. These studies inspired us to ask the following questions: (1) What are the advantages of using NHC and phosphine ligands in the catalysis? (2) What is the rate-determining step for NHC- and phosphine-catalyzed reactions? (3) Does the use of an "abnormal" C5-NHC ligand offer any advantage over normal NHC?

Although the vast majority of NHC−metal binding occurs via the C2 carbon of NHC, there have been a few examples in which NHC uses C5 (**5-IMe**) as the binding site.[36−38] Crabtree et al. and collaborators have shown that C2 to C5 coordination of NHC in complexes can be switched by changing the involved counterions. Recently, Nolan et al. reported on the catalytic role played by the unusual NHC−metal complex, in which the C5 binding to the metal center was formed, instead of the commonly believed C2 binding (imidazol-2-ylidene, **IMe**).[39] Studies using the 5-carbene-Ir complexes suggested that the abnormal NHC is more σ-donating than NHC.[36,37] These findings urged us to compare the catalytic capacity of two types of NHC and phosphine ligands. In our study, we examined the "classical" mechanism, as illustrated in Scheme 1, utilizing realistic model compounds and were able to investigate the complete neutral and ionic reaction pathways. We expected that the free-energy

(22) Herrmann, W. A.; Elison, M.; Fischer, J.; Kocher, C.; Artus, G. R. J. *Angew. Chem., Int. Ed.* **1995**, *34*, 2371−2374.
(23) Crudden, C.; Allen, D. P. *Coord. Chem. Rev.* **2004**, *248*, 2247−2273.
(24) Tubaro, C.; Biffis, A.; Basato, M.; Benetollo, F.; Cavell, K. J.; Ooi, L.-L. *Organometallics* **2005**, *24*, 4153−4158.
(25) Shi, M.; Qian, H.-X. *Tetrahedron* **2005**, *61*, 4949−4955.
(26) Frey, G. D.; Schütz, J.; Herdtweck, E.; Herrmann, W. A. *Organometallics* **2005**, *24*, 4416−4426.
(27) Albert, K.; Gisdakis, P.; Rosch, N. *Organometallics* **1998**, *17*, 1608−1616.
(28) Deeth, R. J.; Smith, A.; Brown, J. M. *J. Am. Chem. Soc*. **2004**, *126*, 7144−7151.
(29) Siegbahn, P. E. M.; Stromberg, S.; Zetterberg, K. *Organometallics* **1996**, *15*, 5542−5550.
(30) Balcells, D.; Maseras, F.; Keay, B. A.; Ziegler, T. *Organometallics* **2004**, *23*, 2784−2796.
(31) Deeth, R. J.; Smith, A.; Hii, K. K.; Brown, J. M. *Tetrahedron Lett*. **1998**, *39*, 3229−3232.
(32) Amatore, C.; Jutand, A. *Acc. Chem. Res.* **2000**, *33*, 314−321.
(33) von Schenck, H.; Åkermark, B.; Svensson, M. *J. Am. Chem. Soc*. **2003**, *125*, 3503−3508.
(34) Ludwig, M.; Strömberg, S.; Svensson, M.; Åkermark, B. *Organometallics* **1999**, *18*, 970−975.
(35) Crabtree, R. H. *J. Organomet. Chem*. **2005**, *690*, 5451−5457.
(36) Gründemann, S.; Kovacevic, A.; Albrecht, M.; Faller, J. W.; Crabtree, R. H. *J. Am. Chem. Soc.* **2002**, *124*, 10473−10481.
(37) Kovacevic, A.; Gründemann, S.; Miecznikowski, J. R.; Clot, E.; Eisenstein, O.; Crabtree, R. H. *Chem. Commun.* **2002**, 2580−2581.
(38) Chianese, A. R.; Kovacevic, A.; Zeglis, B. M.; Faller, J. W.; Crabtree, R. H. *Organometallics* **2004**, *23*, 2461−2468.
(39) Lebel, H.; Janes, M. K.; Charette, A. B.; Nolan, S. P. *J. Am. Chem. Soc*. **2004**, *126*, 5046−5047.

Scheme 2

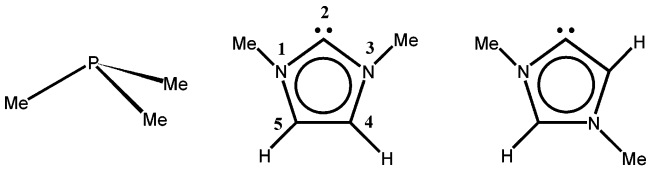

IMe **5-IMe**

profiles of the catalytic cycle would reveal the different natures of the ligands and would provide insights for future studies.

2. Computational Approaches

The theoretical treatment of the systems included in this work was performed using the density functional theory (DFT) approach of the Gaussian03 series of programs. The B3LYP DFT functional was used in this study. B3LYP is a hybrid method that includes Becke's three-parameter mixing of the nonlocal exchange potential[40] and the nonlocal correlation functional of Lee, Yang, and Parr.[41] We used the 6-31G(d) basis sets for the nonmetal atoms. For Pd, we used the relativistic effective core potential (RECP) and basis functions designed by Hay and Wadt.[42,43] The original 3s3p2d basis functions of Hay and Wadt were decontracted to 4s4p3d1f in which an exponent of 1.472 for the f functions was chosen, as suggested by Svensson et al.[44]

Harmonic vibrational frequencies were computed via analytic energy second derivatives at the B3LYP/6-31G(d) level. The frequencies were used to verify whether we have located a genuine minimum and were used to compute zero-point vibrational energy (ZPVE) corrections. At the transition structures, intrinsic reaction coordinate (IRC)[45] computations were performed to verify the connectivity of reactants and products.

The harmonic frequencies were also used to obtain thermal corrections to enthalpy at room temperature and to obtain vibrational entropy. The electronic energy, plus ZPVE, and the energy contributions from translational, rotational, and vibrational motions resulted in the gas-phase enthalpy of a molecule. Similarly, with the inclusion of entropy from translational, rotational, and vibrational motions we obtained Gibbs free energy of a gas-phase molecule.

The solvation free energies were computed using the conductor-like polarizable continuum model (CPCM) of Barone and Cossi.[46] The molecular free energy of the solute embedded in a continuum medium was computed with this method, in which the solute is polarized by the solvent. The approach also allows for the evaluation of the solute−solvent dispersion−repulsion energy. It has been demonstrated that the CPCM model provides predictions for the free energy of hydration that are comparable with experimental results. We have to be aware that in the less coordinated species a solvent molecule can be readily coordinated to the complex and thus our continuum model may not describe the species appropriately. The structures optimized in the gas phase were used in the CPCM calculations. Test cases show that energetics obtained from CPCM-optimized structures are not very different from those obtained using their gas-phase counterparts. We incorporated the dielectric constant of DMSO ($\epsilon = 46.7$) in the CPCM computations. Unless otherwise specified, the energetics discussed in the text are in Gibbs free energies, which include free energy in gas-phase and solvation free energy. Energetics in enthalpies are included in the Supporting Information.

3. Results and Discussion

PdL_2 Complexes. Shortly after Arduengo's isolation of NHC, $Pd^0(NHC)_2$ complexes were isolated.[47−49] By contrast to NHC, Pd^0L_2 complexes of phosphine ligands have not been reported. The optimized structures of $Pd^0(PMe_3)_2$, Pd^0(**IMe**)$_2$, and Pd^0(**IMe**)(**5-IMe**) are shown in Scheme 3 (**1a**−**1c**). The bond angles at the metal center of **1a**, **1b**, and **1c** are 180.0°, 180°, and 179.2°, respectively. In both NHC complexes the five-membered rings are perpendicular. The optimized Pd−C bond distance of 2.048 Å for **1b** is close to the X-ray data for Pd^0(*N*,*N*-di-*tert*-butylimidazol-2-ylidene)$_2$.[47] By comparison with **1b**, the Pd−(**IMe**) bond distance in **1c** is shorter, whereas the Pd−(**5-IMe**) bond distance is longer. At the B3LYP/6-31G(d) level, **5-IMe** is 16.9 and 7.7 kcal/mol higher in energy than **IMe** in the gas phase and in DMSO, respectively. The noticeable difference in solvation free energy can be attributed to the increased gas-phase dipole moment of **5-IMe** (4.7 D) compared to **IMe** (2.7 D). As revealed in our computations, the difference between the solvation free energies of the two ligands primarily comes from the electrostatic term, i.e., the polarized solute−solvent interaction. Similarly, solvation in DMSO favors the abnormal Pd^0(**IMe**)(**5-IMe**) complex (**1c**) by ∼8 kcal/mol. In the gas phase, **1c** lies 16.6 kcal/mol higher in energy than **1b**, while in DMSO the difference is decreased to 8.7 kcal/mol.

Oxidative Addition. Several studies have pointed out that oxidative addition is the rate-determining step.[3] For this reason the oxidative addition product of Pd-catalyzed reactions has been the focus of many studies. Cavell et al. reported the identification of the oxidative addition product of $Pd^0(NHC)_2$ and PhI.[50] Another intermediate has been reported by Caddick, Cloke, and co-workers, in which Pd^0(*N*,*N*-di-*tert*-butylimidazol-2-ylidene)$_2$ reacts with 1-chloro-4-methylbenzene to form *trans*-[Pd^{II}(*N*,*N*-di-*tert*-butylimidazol-2-ylidene)$_2$(4-Me-C_6H_4)Cl].[51]The Pd−NHC dissociation enthalpy of 25.57 kcal/mol was determined via analysis of the temperature dependence of the equilibrium constants.[52] All of these intermediates adopt the *trans* arrangement of two NHCs.

Our computations began with the formation of the PdL_2-bromobenzene adduct (**2a**−**2c**), as evidenced by the L−Pd−L bond angle decrease to approximately 110° in the adduct. Oxidative addition was then completed with a Br migration, resulting in intermediate products **4a′**−**4c′** and the final products **4a**−**4c** (Scheme 4 and Figure 1). For the phosphine system, **4a′** adopts a *trans* ligand arrangement, while for the NHC system **4b′** and **4c′** adopt a *cis* ligand arrangement. In *cis* complexes the two Pd−L distances are not equivalent as a consequence of the *trans* influence. Bond distances of Pd−L *trans* to the phenyl group are relatively longer than those of the *cis* ones. In the

Scheme 3

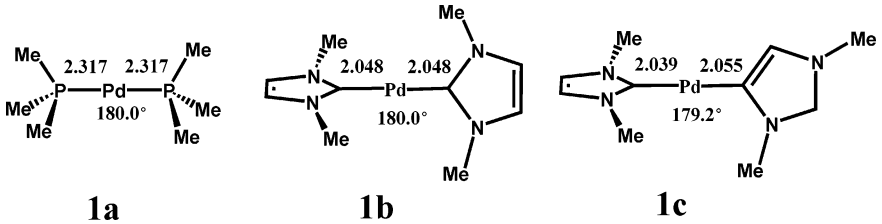

1a **1b** **1c**

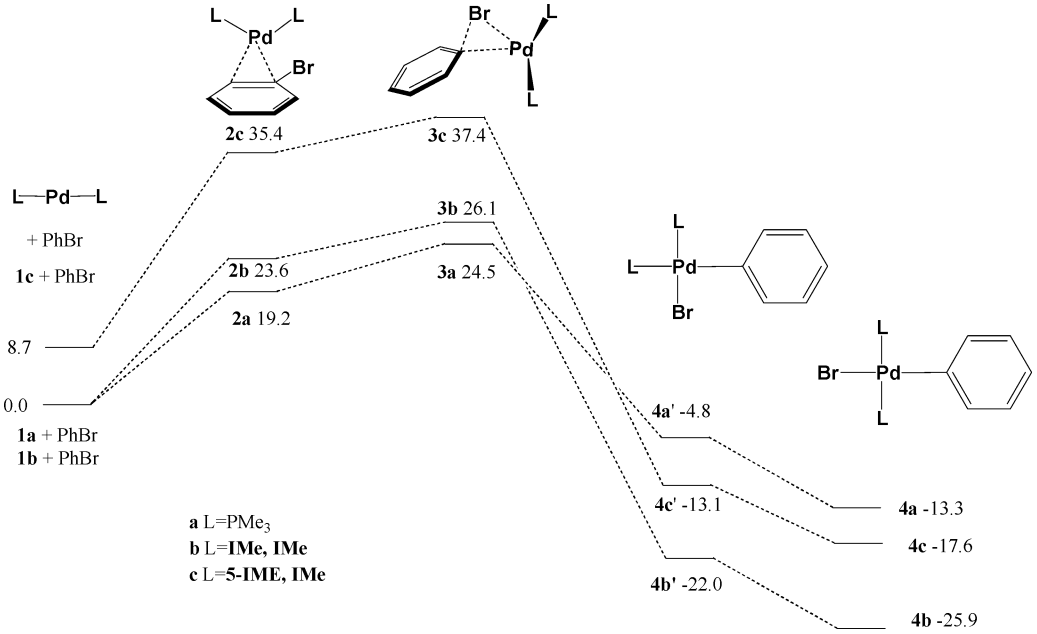

Figure 1. Free-energy profile of the oxidative addition step computed with the CPCM model (DMSO). Note that **4a** adopts *cis* form and **4a′** adopts a *trans* form; see text.

Scheme 4

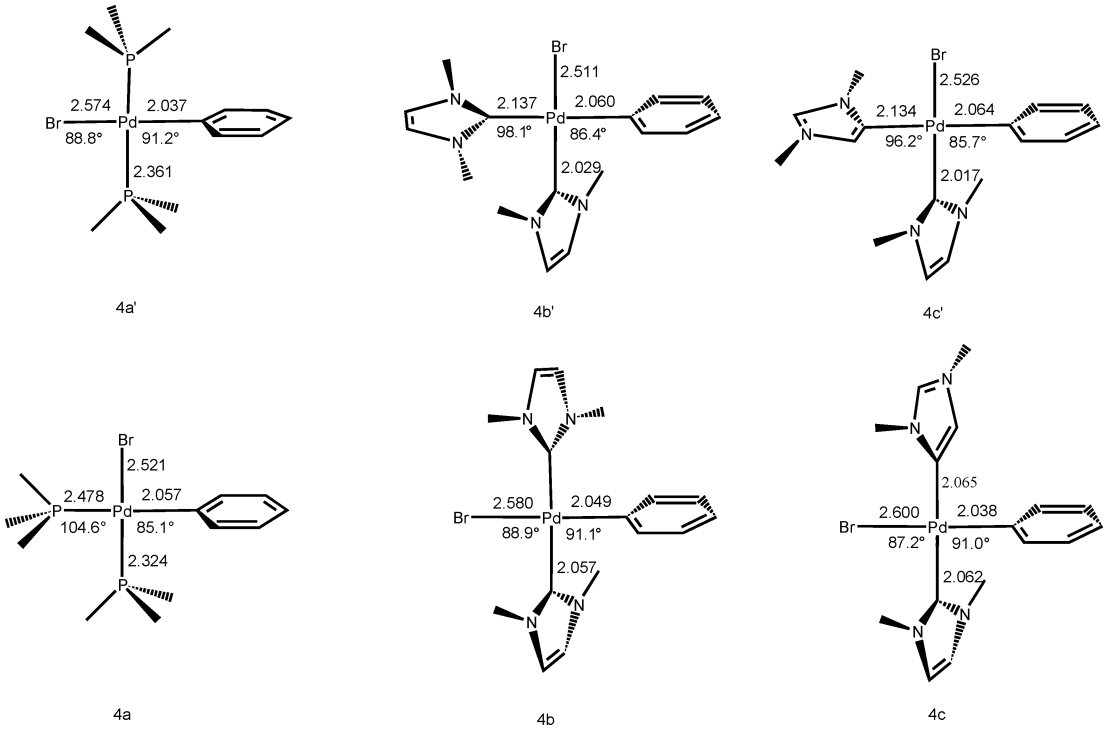

case of **4a**, the bond distance is 2.478 versus 2.324 Å, and in the case of **4b**, the bond distance is 2.137 versus 2.029 Å. In **4c′** the conformer in which **5-IMe** adopts a *trans* arrangement to the phenyl group is lower in energy, and its geometrical parameters are shown in Scheme 4. It is worth mentioning that in **4b′** and **4c′** the two five-membered rings and the phenyl ring are approximately vertical with respect to the square plane, and the geometrical arrangement is similar to that reported for Pd^{II}-

(40) Becke, A. D. *J. Chem. Phys.* **1993**, *98*, 5648−5652.
(41) Lee, C.; Yang, W.; Parr, R. G. *Phys. Rev. B* **1988**, *37*, 785−789.
(42) Hay, P. J.; Wadt, W. R. *J. Chem. Phys.* ***1985***, *82*, 299−310.
(43) Hay, P. J.; Wadt, W. R. *J. Chem. Phys.* **1985**, *82*, 284−298.
(44) von Schenck, H.; Akermark, B.; Svensson, M. *Organometallics* **2002**, *21*, 2248−2253.
(45) Gonzalez, C.; Schlegel, H. B. *J. Phys. Chem.* **1990**, *94*, 5523−5527.
(46) Barone, V.; Cossi, M. *J. Phys. Chem. A* **1998**, *102*, 1995−2001.
(47) Arnold, P. A.; Cloke, F. G. N.; Geldbach, T.; Hitchcock, P. B. *Organometallics* **1999**, *18*, 3228−3233.
(48) Arentsen, K.; Caddick, S.; Cloke, F. G. N.; Herringc, A. P.; Hitchcock, P. B. *Tetrahedron Lett.* **2004**, *45*, 3511.
(49) Gstöttmayr, C. W. K.; Böhm, V. P. W.; Herdtweck, E.; Grosche, M.; Herrmann, W. A. *Angew. Chem., Int. Ed.* **2002**, *41*, 1363−1365.
(50) McGuinness, D. S.; Cavell, K. J.; Skelton, B. W.; White, A. H. *Organometallics* **1999**, *18*, 1596−1605.
(51) Caddick, S.; Cloke, F. G. N.; Hitchcock, P. B.; Leonard, J.; Lewis, A. K. d. K.; McKerrecher, D.; Titcomb, L. R. *Organometallics* **2002**, *21*, 4318−4319.
(52) Lewis, A. K. d. K.; Caddick, S.; Cloke, F. G. N.; Billingham, N. C.; Hitchcock, P. B.; Leonard, J. *J. Am. Chem. Soc.* **2003**, *125*, 10066−10073.

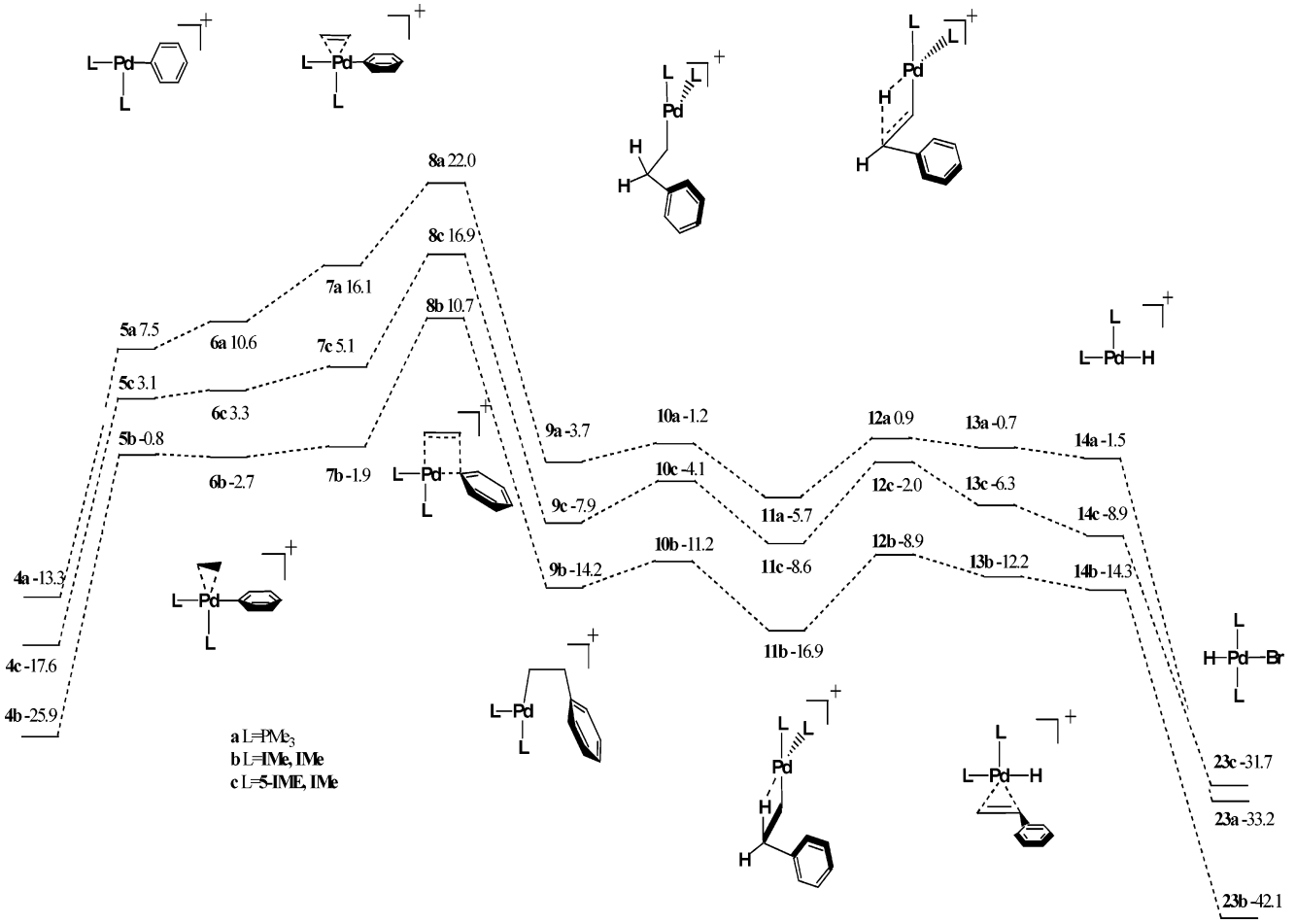

Figure 2. Free-energy profile of the cationic path, including olefin insertion, and the β-hydride elimination steps computed with the CPCM model (DMSO). Refer to the Supporting Information for detailed geometrical arrangements.

(**IMe**)$_2$I$_2$ by Hermann et al.[22] The more stable species **4a**−**4c** have been identified as the products of our IRC computations using transition structures **3a**−**3c**. This observation suggests that the transition from **4a′**−**4c′** to **4a**−**4c** may readily occur.

The energy profile in Figure 1 shows that oxidation addition of the NHC system is a very exothermic step. For the phosphine system, the reaction is much less exothermic than those for the NHC systems. The activation barrier for the phosphine system is smaller than those of the NHC systems. For the NHC systems, the **1c**−**3c** barrier is 2.6 kcal/mol larger than that of **1b**−**3b**.

An alternative mechanism leading to the formation of the *trans* complex is the predissociation of one ligand from **1**, followed by oxidation addition and the recoordination of the ligand. However this reaction path was not included in our study.

The ligand−Pd bond strength of NHC in complexes such as **4** are significantly stronger than that of phosphine. The gas-phase ligand−Pd bond dissociation enthalpies for **4a**−**4c** are 32.9, 55.4, and 55.3 kcal/mol, respectively. In solution (DMSO), the free energies of ligand dissociation are 20.1, 34.6, and 37.4 kcal/mol for **4a**−**4c**, respectively. The marked difference between the bond strengths of NHC and phosphine suggests that in the olefin insertion step, NHC systems are less likely to undergo the neutral pathway (vide infra).

Olefin Insertion and β-Hydride Elimination. At this stage of the reaction, a three-coordinate complex is formed from the oxidative oxidation product. Neutral and cationic complexes can be generated, depending on the dissociation of a ligand (neutral path) or halide anion (cationic path). Evidence of the existence of neutral three-coordinate intermediates has been reported in several experimental studies.[52,53] Even though oxidative addition is considered the rate-determining step in many instances,[3] there are examples that suggest that olefin insertion is the rate-determining step.[54]

Ionic Pathway. In the cationic pathway, gas-phase computation for the dissociation of Br$^-$ from the oxidative addition complex is unrealistic since it neglects the solvation effects. With respect to the *trans* oxidation addition products **4a**−**4c**, the free energy of dissociation of Br$^-$ into **5a**−**5c** in DMSO requires 20.8, 25.1, and 20.7 kcal/mol, respectively. It appears that the presence of C5-metalated NHC (**5c**) facilitates the dissociation of the bromide ion compared with the C2-metalated NHC (**5b**). The dissociation of Br$^-$ for **5c** occurs more easily. As expected, the dissociation free energy of the bromide ion is very sensitive to the solvent. Our computation shows that with the less polar solvent (THF) there is an increase of about 10 kcal/mol for the dissociation free energy. It is noted, however, that in the ionic pathway the solvation free energies of the ionic species are more than 100 kcal/mol higher than those of the neutral species (see Supporting Information).

Due to the entropy loss, ethylene addition is not a very favorable process. In fact, when ethylene attaches to **5b**, the adduct (**6b**) is only 1.7 kcal/mol lower in energy. The adduct **6c** is slightly less favorable than **5c** by 0.2 kcal/mol, while that of **6a** is more unfavorable than **5a** by 3.1 kcal/mol (Figure 2).

(53) Stambuli, J. P.; Bühl, M.; Hartwig, J. F. *J. Am. Chem. Soc*. **2002**, *124*, 9347−9348.

(54) van Strijdonck, G. P. F.; Boele, M. D. K.; Kamer, P. C. J.; de Vries, J. G.; van Leeuwen, P. W. N. M. *Eur. J. Inorg. Chem.* **1999**, 1073−1076.

Scheme 5

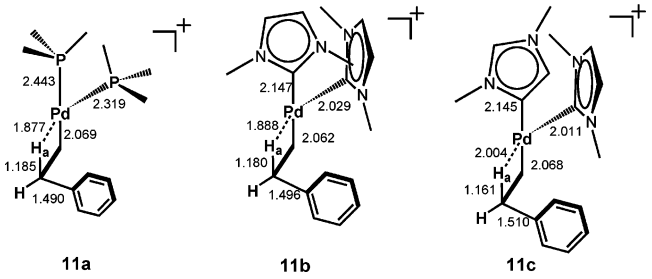

For adducts **6a**−**6c**, ethylene adopts a perpendicular rearrangement with respect to the Pd^0L_2 plane. Prior to the phenyl migration, the ethylene moiety has to adopt a parallel arrangement (**7a**−**7c**). For NHC systems, ethylene almost freely rotates to the parallel arrangement, while it requires more energy for the phosphine system (**7a**) to rotate. The phenyl group then migrates to ethylene, forming the three-coordinate species with the $-CH_2CH_2Ph$ group on Pd (**9a**−**9c**). Along the reaction coordinate the transition states of the migration adopt a four-membered ring arrangement in which both the Pd^{II}−C(Ph) bond and ethylene C−C bonds are lengthened. The transition states corresponding to the phenyl migration, **8a**−**8c**, are the highest points on the free-energy profile in Figure 2 and are 35.3, 36.6, and 34.5 kcal/mol above **4a**−**4c**, respectively. By contrast to the C2-NHC system, the abnormal C5-NHC system exhibits a slightly lower barrier (2.1 kcal/mol).

Before the β-hydride elimination step, the three-coordinate complexes **9a**−**9c** must rearrange to a geometry where Pd^{II}−C−C−H_a (H_a: agostic hydrogen) is close to planar. The Pd^{II}−C−C−H_a dihedral angles for **9a**−**9c** are in the range of 88−101° compared to 42−52° at the TS (**10a**−**10c**), and finally in the rotated isomers (**11a**−**11c**), the dihedral angles are 4−8°. The distance between Pd^{II} and the agostic hydrogen is about 1.98−2.00 Å, and the C−H_a distance is noticeably longer than that of a nonagostic hydrogen. As shown in Figure 2, **9a**−**9c** experience a small energy barrier upon rotation of the Pd−C bond, and the complexes **11a**−**11c** are stabilized via Pd−H interaction. As shown in Scheme 5, the C−H_a bond is noticeably lengthened and the Pd−H_a distance is only 1.88−2.00 Å. β-Hydride elimination then occurs from this point, forming complexes **13a**−**13c**, followed by the dissociation of styrene (**14a**−**14c**) and the reattachment of bromide (**23a**−**23c**). In contrast to the olefin insertion process, β-hydride elimination occurs with little change in free-energy profile (Figure 2). Very recently, a palladium hydride $L_2Pd^{II}HCl$ has been identified in Fu's laboratory.[55]

At this point we would like to make comparisons between our results and those of previous theoretical studies. In the theoretical study of Siegbahn et al., the olefin insertion step involved the insertion of ethylene to $Pd^{II}(NH_3)_2C_2H_5^+$ and related complexes.[29] The migration energy barrier for the olefin adduct was predicted to be about 16−19 kcal/mol. The migration process was predicted to be exothermic, followed by low-barrier β-hydride elimination, which was slightly endothermic. Our energy profile in Figure 2 (**5** → **13**) resembles these results. A marked difference is that olefin coordination was very exothermic in the previous theoretical study, while with the inclusion of both solvation and entropy effects we found that the free energies of complexes **6** are rather similar to those of **5**, plus free ethylene. Overall, our prediction of the free-energy profile for β-hydride elimination agrees with previous studies, i.e., the process has a very flat energy profile.

A DFT study by Ziegler et al. investigated the use of bidentate phosphine ligands and explored, in detail, the mechanism of Pd^{II}-assisted copolymerization of ethylene and CO.[56] In this study, attempts to locate the energy minimum of olefin coordination adduct $Pd^{II}(PH_2CH{=}CHPH_2)(H)(C_2H_4)^+$ invariably resulted in the β-agostic compound (analogue of **11a**). By contrast, we found that complexes **6a** and **7a** are genuine minima, attributable to the different electronic nature between the H atom and the phenyl ring. Our free-energy profile also differs from that obtained by Deeth et al. using DFT.[31] Using $H_2PCH_2PH_2$ as ligand, the β-hydride elimination product (the analogue of **13a**) was not located. In this study the authors examined the $HPdL_2^+$ cation (the analogue of **14a**) and found that it is not a local minimum. Only the β-agostic complex (the analogue of **11a)** was located by the authors. This observation led the authors to propose that the base elimination pathway begins directly from **11a**. On the other hand, our computation shows that **13a** is a genuine minimum. When compared to the phosphine system, the NHC systems **13b** and **13c** are less likely to be converted back to the β-agostic complexes **11b** and **11c**.

Neutral Pathway. In addition to the aforementioned cationic pathway, the catalytic cycle could occur through dissociation of one ligand from complexes **4a**−**4c**, i.e., via the neutral pathway with $Pd^{II}LPhBr$ (**15a**−**15c**), which are formed by the exclusion of one ligand (PMe_3 or **IMe**). In **15c**, **IMe** is dissociated from **4c**. As shown in Figure 3, removal of PMe_3 and **IMe** from **4a**−**4c** requires 20.1, 34.6, and 37.4 kcal/mol for **4a**−**4c**, respectively. Since the NHC−Pd bond is stronger than that of the phosphine complex, removal of **IMe** requires more energy than for PMe_3. The marked difference between the bond strengths of NHC and phosphine suggests that NHC systems are much less likely to undergo the neutral pathway.

Similar to the ionic pathway, ethylene attaches to the three-coordinate complexes and forms **16a**−**16c**. These complexes then overcome a barrier (**17a**−**17c**) of ∼10 kcal/mol and form the three-coordinate complexes **18a**−**18c**. One noteworthy point is that our **18a** shares a very similar geometry with $Pd^{II}(CH_2CMe_2Ph)(PMe_3)OTf$, which was synthesized by Cámpora et al.[57] The isomers of the three-coordinate complexes **18a**−**18c**, which possess Br *trans* to the phenyl group, have been located. These species are ∼8 kcal/mol higher in energy than **18a**−**18c** and thus will not be discussed further. Another geometrical arrangement in which the ligands and bromide possess *trans* positions has also been located (**19a**−**19c**).

Unlike the ionic pathway, direct β-hydride elimination does not occur, and instead, the dissociated ligand reattaches to the complex, forming **20a**−**20c**. As shown, the NHC systems are more stabilized by the addition of ligands than the phosphine system (**20a**−**20c**). β-Hydride eliminations then occur via transition states **21a**−**21c**, resulting in the five-coordinate complexes **22a**−**22c**, from which the olefin easily dissociates (to **23a**−**23c**). The overall energy profile in Figure 3 reveals that the neutral path is much more favored for the phosphine system. One important advantage is that in the phosphine system the ligand readily dissociates (**4a** → **5a**). An additional advantage of phosphine system is that its migration product (**20a**) lies higher in energy on the free-energy profile; thus it experiences a smaller barrier in β-hydride elimination.

(55) Hills, I. D.; Fu, G. C. *J. Am. Chem. Soc.* **2004**, *126*, 13178−13179.

(56) Margl, P.; Ziegler, T. *J. Am. Chem. Soc.* **1996**, *118*, 7337−7344.

(57) Cámpora, J.; López, J. A.; Palma, P.; Valerga, P.; Spillner, E.; Carmona, E. *Angew. Chem., Int. Ed.* **1999**, *38*, 147−151.

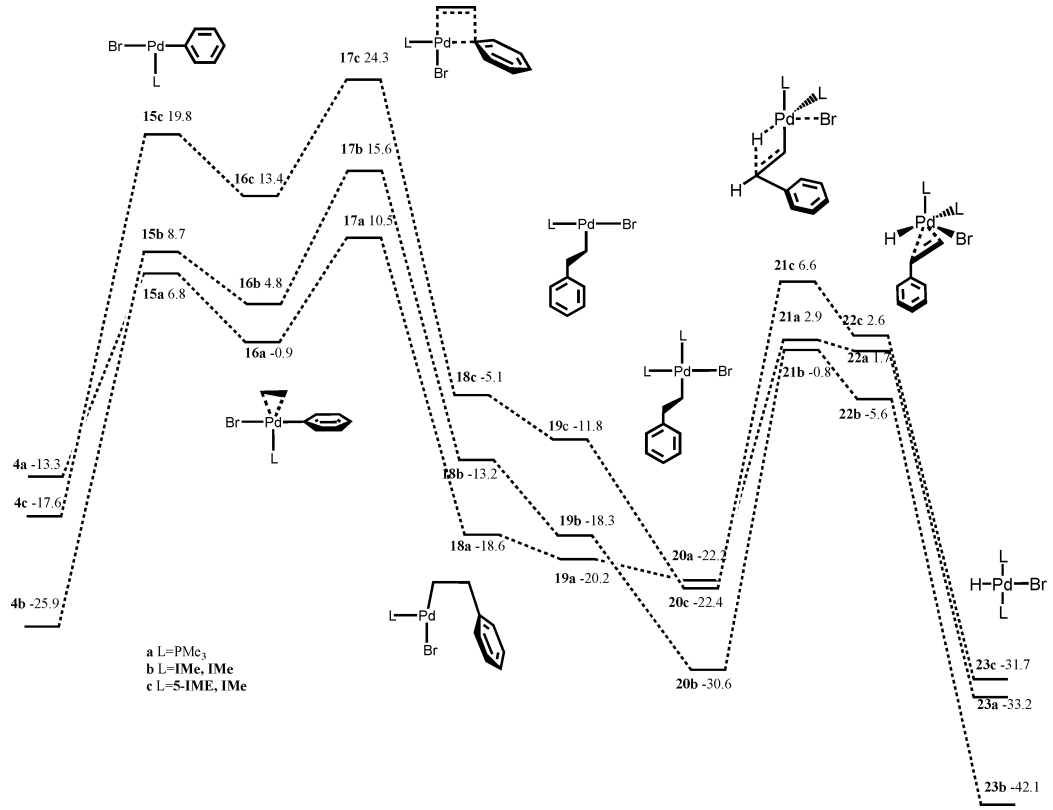

Figure 3. Free-energy profile of the neutral path, including olefin insertion, and the β-hydride elimination steps computed with the CPCM model (DMSO). Refer to the Supporting Information for detailed geometrical arrangements.

Base Elimination of HBr and the Overall Free-Energy Profile. In the last step of the reaction cycle, base is involved to remove HBr from the $L_2Pd^{II}HBr$ complex. Compared with the previous steps, base elimination has not received as much attention. A recent mechanistic study by Fu et al. reveals, however, that the catalytic capacity of the Heck reaction in phosphine system depends upon the efficiency of base elimination from $L_2Pd^{II}HCl$.[55]

There are several mechanistic possibilities for the base elimination step. Base can assist the migration of hydrogen during the $L_2Pd^{II}HBr \rightarrow Pd^0L_2$...(HBr) reaction, or the base can bind to the complex before intramolecular rearrangement into Pd^0L_2...(R_3NHBr). A previous theoretical study by Deeth et al. suggests that base directly removes the proton from **11a**, thereby completing the catalytic cycle.[31] The base applied in the study Deeth et al. was a neutral one. In some cases, an ionic base can be used for proton elimination. Examination of these possibilities is a formidable task, and since it is generally accepted that base elimination is not the crucial step, we chose to compute the free energy of reaction using the following reaction:

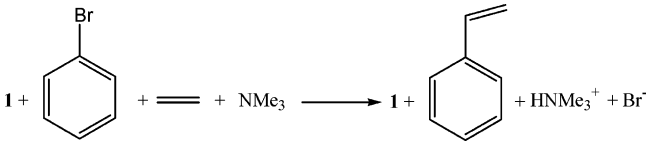

Our computations, utilizing a 6-311++G(d,p) basis set for the electronic energy and solvation free energy, plus the enthalpy and free-energy correction using the 6-31G(d) basis set, resulted in a free energy of reaction of −33.0 kcal/mol. The relative energies of **1a**−**1c** after one catalytic cycle are thus −33.0, −33.0, and −24.3 kcal/mol, respectively. From this point of view, the reaction should be viewed as a cascade of consecutive energy profiles as illustrated in Figure 4.

Caution should be taken when interpreting the mechanism described above. Direct comparison of the cationic versus neutral pathways may not be appropriate, as the solvation free energy for the dissociation of bromide (**4** → **5**) in the ionic pathway is about 90 kcal/mol, while that of the neutral path (**4** → **15**) is only a few kcal/mol. When we used a larger basis set, [6-311++G(d,p)], the energy profile of the **4** → **5** dissociation was decreased by ∼10 kcal/mol, while that of the ligand dissociation **4** → **15** did not significantly change.

4. Conclusion

In this study, we presented the free-energy profile of the Heck reaction as computed using density function theory. The model compounds we used were more realistic than those utilized in previous theoretical approaches. In addition, the solvation free energy of DMSO was included via the conductor-like polarizable continuum model (CPCM). Our study shows that oxidative addition has a very high energy barrier, and oxidative addition occurs much more easily for the phosphine system. The activation barrier for the oxidative addition of the C2-NHC system is slightly lower than that for the C5-NHC system. The oxidative addition process is, at least, one of the rate-determining steps during a catalytic cycle. For the ionic pathway, the other rate-determining step is olefin migration (**8a**−**8c**). For the neutral pathway, the rate-determining step is also olefin migration for NHC systems (**17b**,**17c**). For the phosphine system, olefin migration appears to be much easier. Our result suggests that the phosphine system favors the neutral pathway. For all the systems studied, the β-hydride elimination step experiences a very flat free-energy profile. The catalytic capacity of Pd^0L_2 involving the "abnormal" C5-NHC ligand (**5-IMe**) is similar to the regular C2-NHC ligand. Despite the many applications of NHC, in the textbook mechanism of the Heck reaction there is no obvious advantage of its usage.

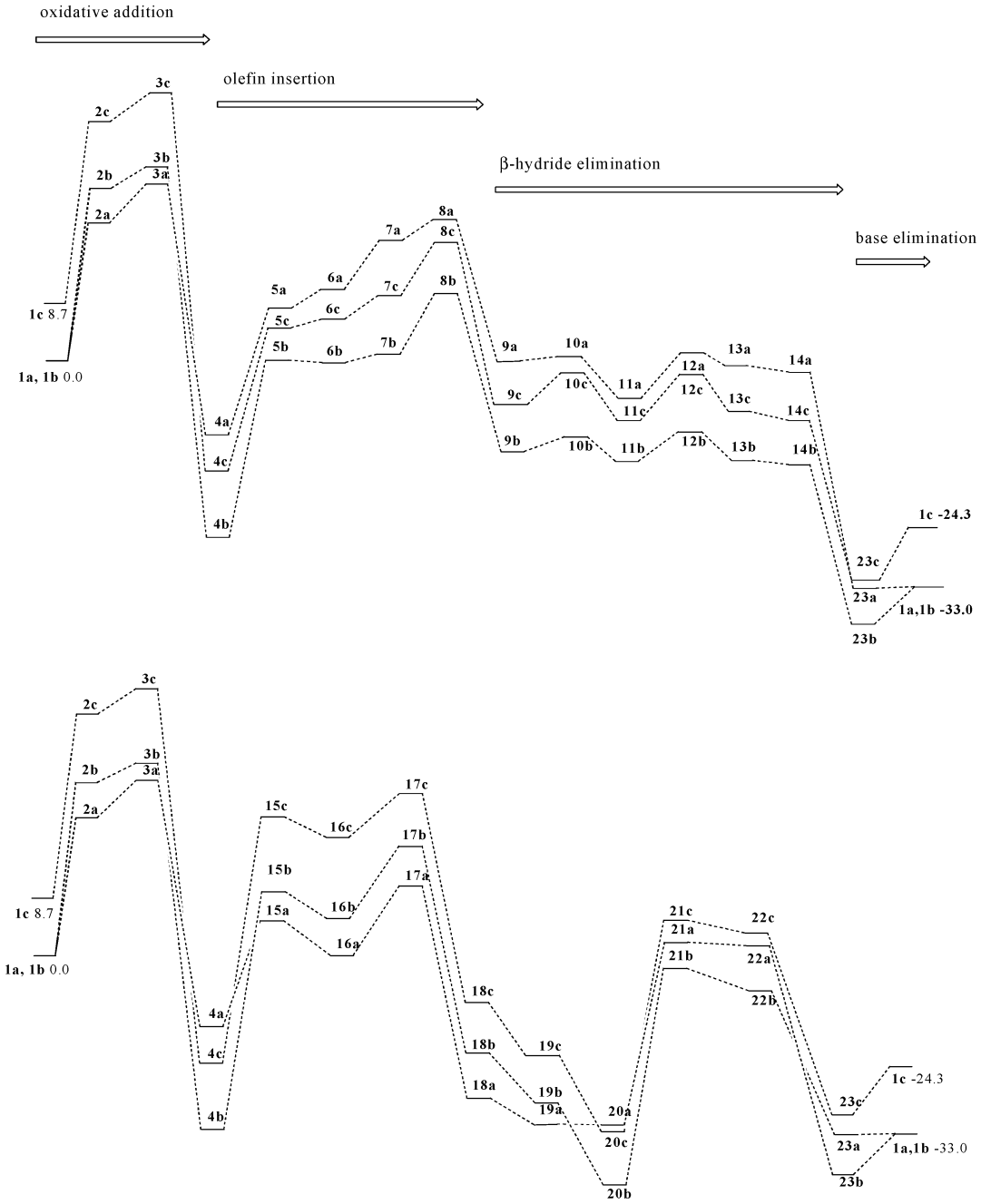

Figure 4. View of the free-energy profiles of cationic (above) and neutral (below) paths. The energies of **1a** and **1b** are set to zero.

Acknowledgment. The authors acknowledge that the National Science Council of Taiwan, Republic of China, supported this work. We also thank the National Center for High-Performance Computing for computer time and facilities.

Supporting Information Available: Cartesian coordinates of stationary points, IRC data, illustrated geometries and important geometrical parameters, magnitude of imaginary frequencies of transition states, and energetics including relative enthalpies and free energies in both the gas-phase and DMSO are available, free of charge, via the Internet at http://pubs.acs.org.

OM060651P